3

Electrochemical carbon dioxide and bicarbonate reduction on copper in weakly alkaline media

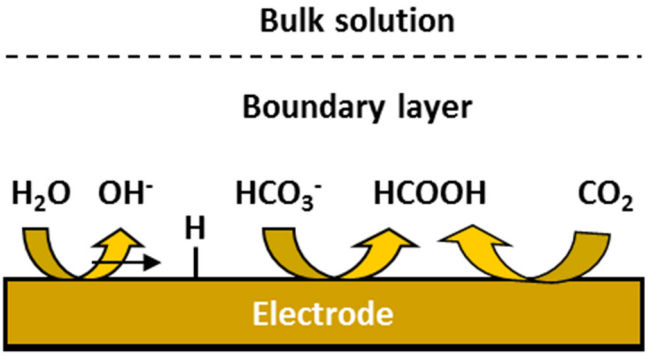

The contents of this chapter have been published as: R. Kortlever, K.H. Tan, Y. Kwon and M.T.M. Koper, *J. Solid State Electrochem.* **2013**, *17*, 1843-1849.

Abstract The electrochemical reduction of CO_2 on copper is an intensively studied reaction. However, there has not been much attention for CO_2 reduction on copper in alkaline electrolytes, because this creates a carbonate buffer in which CO_2 is converted in HCO_3^- and the pH of the electrolyte decreases. Here we show that electrolytes with phosphate buffers which start off in the alkaline region and, after saturation with CO_2, end up in the neutral region, behave differently compared to CO_2 reduction in phosphate buffers which start off in the neutral region. In initially alkaline buffers a reduction peak is observed, which is not seen in neutral buffer solutions. In contrast with earlier literature reports we show that this peak is not due to the formation of a CO ad-layer on the electrode surface but due to the production of formate via direct bicarbonate reduction. The intensity of the reduction peak is influenced by electrode morphology and the identity of the cations and anions in solution. It is found that a copper nanoparticle covered electrode gives a rise in intensity in comparison with mechanically polished and electropolished electrodes. The peak is observed in SO_4^{2-}, ClO_4^- and Cl^- containing electrolyte, but the formate-forming peak is not seen with Br^- and I^-.

3.1 Introduction

The emission of CO_2 into the atmosphere, causing a green-house effect, has led to increasing interest in developing new energy sources. Closing the anthropogenic carbon cycle by using renewable energy to electrochemically reduce CO_2 into fuels is one of the options.[1,2]

Ever since Hori's discovery[3] in 1985 that copper can electrochemically reduce CO_2 to hydrocarbons, there has been a lot of research to further investigate the possibilities of this reaction.[4-7] However, these studies were mostly limited to acidic and neutral aqueous electrolytes, while alkaline electrolytes were neglected. The reason for this is that once an alkaline electrolyte is purged with CO_2, a carbonate buffer is created lowering the pH value of the solution via the following equilibria:

$$CO_2 + H_2O \leftrightarrows H_2CO_3 \quad (1)$$

$$H_2CO_3 \leftrightarrows HCO_3^- + H^+ \qquad pK_{a2} = 6.35\ (25\ ^oC) \quad (2)$$

$$HCO_3^- \leftrightarrows CO_3^{2-} + H^+ \qquad pK_{a3} = 10.33\ (25\ ^oC) \quad (3)$$

These equilibria show that the total amount of carbonaceous species that can be dissolved in water increases with pH from ca. pH = 5.5. More interesting from the catalytic point-of-view, the selectivity of CO_2 reduction might depend on pH. Recently, our group showed that for CO reduction, which is a key step in CO_2 reduction, the onset potential for ethylene formation was dependent on the pH of the electrolyte: for an alkaline electrolyte the onset potential for ethylene formation was significantly lower than for a neutral electrolyte.[8] Furthermore, experiments by Hori et al. have shown that the formation of methane is dependent on pH, since it requires the simultaneous transfer of a proton and an electron in the rate-determining step. The formation of ethylene however is independent of pH, since its rate-determining step only requires the transfer of an electron.[9] Therefore one can expect that product selectivities in weakly alkaline media will differ from neutral and acidic media.

In this chapter, electrochemical CO_2 reduction on copper in neutral phosphate buffers will be compared to CO_2 reduction in phosphate buffers that started at an alkaline pH before bubbling CO_2 through the electrolyte. In addition, the influence of different cations and anions on the reduction of CO_2 in phosphate buffers was investigated. The electrochemical reactions were studied using cyclic voltammetry, online mass spectroscopy (OLEMS) and online high-performance liquid chromatography (HPLC).

3.2 Experimental

All electrochemical experiments were carried out in an electrochemical cell using a three-electrode assembly at room temperature. The cell and all other glassware were first cleaned by boiling in a 1:1 mixture of concentrated sulfuric and nitric acid and were cleaned before every experiment by boiling in ultra-pure water

(Millipore MilliQ gradient A10 system, 18.2 MΩ cm). A coiled gold wire was used as counter electrode. All potentials are reported versus the reversible hydrogen electrode (RHE) as reference electrode in a separate compartment filled with the same electrolyte, at the same pH as the electrolyte in the electrochemical cell. Since the pH of the electrolyte, including that of the reference compartment, can change, all voltammetric measurements were scanned to values where the copper oxidation and copper oxide reduction peaks are included in the scan, so as to provide an extra reference point for the electrode potential.

A cylindrical polycrystalline copper electrode (99.999% Cu, purchased at Mateck GmbH) with a diameter of 5 mm embedded in teflon was used as working electrode. Prior to every experiment the work electrode was polished mechanically to a mirrorlike finish using alumina pastes. After this, the electrode was sonicated in ultra-pure water. If mentioned, electrodes were electropolished in a 65% solution of H_3PO_4 in ultra-pure water at 3 V for 10 s. Cyclic voltammograms at a scan rate of 20 mV s^{-1} were recorded on an Ivium A06075 potentiostat. Single crystal experiments were performed with bead single crystal copper electrodes, purchased from icryst, in a hanging meniscus setup. Before use the single crystals were electropolished in the same manner as mentioned above. A blank cyclic voltammogram in 0.1 M NaOH was recorded to characterize the single-crystal electrode surface and the blank voltammograms were compared with published voltammograms.[8,10]

Electrolytes were made from ultra-pure water and high purity reagents (Merck Suprapur, Sigma Aldrich TraceSelect). Before each experiment the electrolytes were first purged with Argon (Air Products, 5.0) for 15 minutes to remove air from the solution, after which they were purged with CO_2 (Linde, 4.5) for 30 minutes to saturate the solutions.

Online Electrochemical Mass Spectrometry (OLEMS) was used to detect gaseous products of the reactions. The products were collected with a small hydrophobic tip which was positioned close (about 10 µm) to the electrode with the aid of a camera.[11] The tip was constructed as a porous Teflon cylinder with a diameter of 0.5 mm and an average pore size of 10-14 µm in a Kel-F holder. The tip is connected to a mass spectrometer with a PEEK capillary. Before use the tip

was cleaned in a solution of 0.2 M $K_2Cr_2O_7$ in 2 M H_2SO_4 and rinsed thoroughly with Millipore water. A secondary electron multiplier (SEM) voltage of 2400 V was used for detection in a Balzers Quadrupole mass spectrometer, except for hydrogen (m/z = 2) where a SEM voltage of 1200 V was used. The products were measured while changing the potential of the electrode from 0.0 V to -1.0 V and back at 1 mV s^{-1}.

Products dissolved in the electrolyte were detected using online High Performance Liquid Chromatography (HPLC).[12] While changing the potential from 0.0 V to -1.0 V, samples were collected with an open tip positioned close (~10 µm) to the electrode. Sampling was done at a rate of 60 µL min^{-1} and each sample had a volume of 60 µL. Since the potential was changed at 1 mV s^{-1}, each sample contained the average products of a potential change of 60 mV. After the voltammetry, these samples were analyzed by HPLC (Prominence HPLC, Shimadzu; Aminex HPX 87-H column, Biorad).

3.3 Results and discussion

3.3.1 Observation of a reduction peak in electrolytes starting at alkaline pH

When CO_2 reduction on a polycrystalline copper electrode in different pH buffers was studied with cyclic voltammetry, we saw a difference in the voltammograms of phosphate buffer solutions starting at different pH's (Figure 3.1). In the voltammogram corresponding to a phosphate buffer starting at pH 11.6 a reduction peak is seen at -0.6 – -0.7 V vs. RHE while in the other voltammograms, corresponding to phosphate buffers starting at pH 2 and at pH 6.7, no such peak is observed. This peak was also observed if 0.1 M KOH (with a start pH 12, which shifted to pH 7.5 after purging with CO_2 for 30 min.) was used as electrolyte, but in that electrolyte the peak had a lower intensity. The reduction peak is thus not due to the phosphate species in the electrolyte, but clearly dependent on the

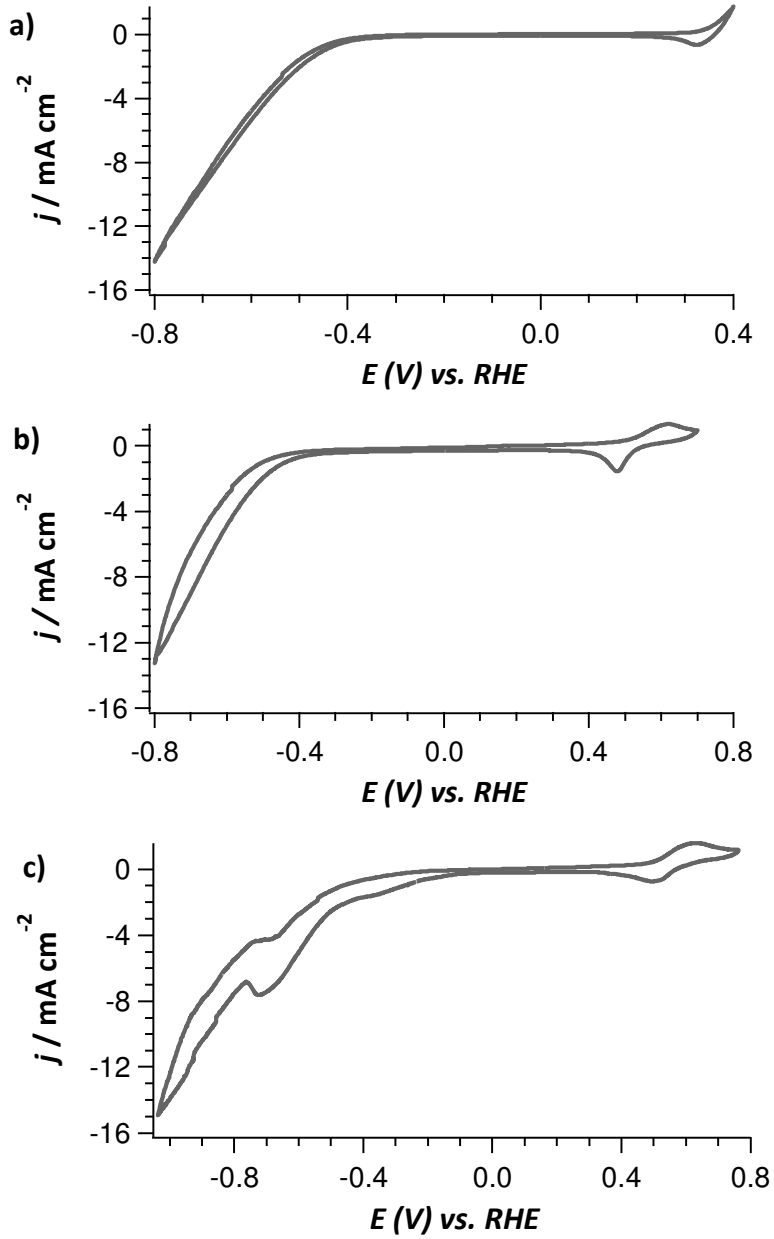

Figure 3.1 Comparison of cyclic voltammograms of CO_2 reduction on polycrystalline copper with different phosphate buffers as electrolyte at a scan rate of 20 mV s^{-1}. **a)** 0.1 M KH_2PO_4 / 0.1 M H_3PO_4 (pH = 2.0), **b)** 0.1 M KH_2PO_4 / 0.1 M K_2HPO_4 (pH = 6.7), **c)** 0.1 M K_2HPO_4 / 0.1 M K_3PO_4 (pH = 11.6).

starting pH of the electrolyte. We also note that the cathodic current in Fig. 3.1a-c is mainly due to H_2 evolution, as the difference between the reduction current between the blank and the solution with CO_2 is very small (as is well known[6]). However, the peak is not observed without CO_2 in solution.

A similar reduction peak was observed by Hori et al.,[14,15] and has also been described in later as well as more recent voltammetric studies.[15,16] These authors observed this peak in a phosphate buffer (0.05 M KH_2PO_4 + 0.15 M K_2HPO_4) and in 0.5 M $KHCO_3$ respectively. Since the phosphate buffers used by us and also by Hori et al. are alkaline, a carbonate buffer will form in the electrolyte as explained in the Introduction. This results in a decrease of the pH of the solution, from pH 11.6 to approximately pH 7.6 measured after CO_2 purging and subsequent reduction. The reduction peak was ascribed to the formation of a layer of adsorbed CO in the literature,[13] which is an intermediate product of CO_2 reduction on copper. This CO ad-layer would suppress the hydrogen evolution reaction that competes with CO_2 reduction for adsorption spots on the surface of the catalyst. On the other hand, reported faradaic efficiencies (and thus production rates) of the formation of hydrogen in a K_2HPO_4 solution are significantly higher than for other electrolytes as K_2SO_4, $KClO_4$ and KCl (72.4% vs.

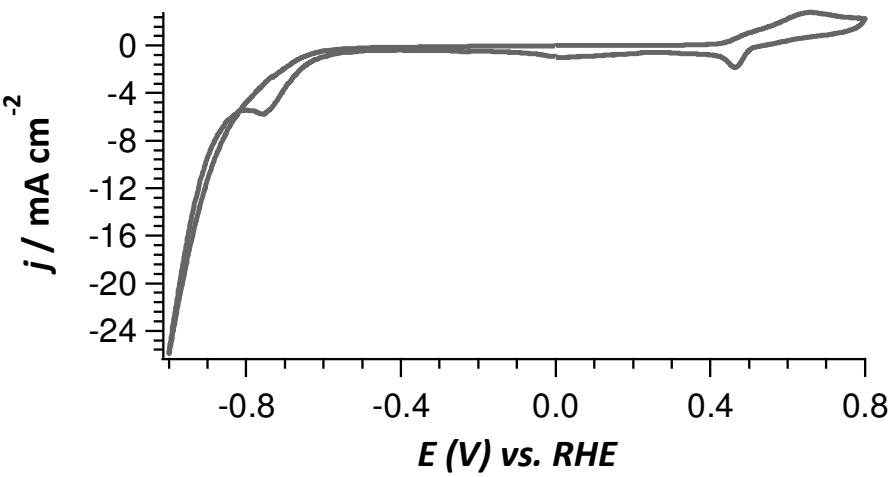

Figure 3.2 Cyclic voltammogram of a polycrystalline copper electrode in a 1.0 M $KHCO_3$ electrolyte at a scan rate of 20 mV s^{-1}.

8.7%, 6.7% and 5.9% respectively),[13] suggesting that CO adsorption does not play a major role.

The difference between the two buffer solutions does not lie so much in the values of the pH after purging CO_2 through the respective solutions, but rather in the amount of CO_2 converted into HCO_3^-, that is related to the initial pH of the electrolyte. To investigate if the peak was due to direct bicarbonate reduction, as has been observed earlier on palladium electrodes,[17,18] a cyclic voltammogram was recorded in a 1.0 M $KHCO_3$ electrolyte (Figure 3.2). A similar reduction peak as to the electrolyte in Figure 3.1c is observed. This implies that bicarbonate can be readily reduced on copper, like on palladium. Previous studies often stated that CO_2 and not HCO_3^- is the reducible species,[19] Hori and Suzuki concluded that the electrochemical reduction of HCO_3^- is a very slow process, due to the slow dissociation of HCO_3^-:[20]

$$HCO_3^- \rightarrow CO_2 + OH^- \quad (5)$$

However, on palladium it has been claimed that bicarbonate is reduced via a direct reduction.[21] This pathway would directly reduce bicarbonate to formate without the need for bicarbonate to dissociate to CO_2 in solution:

$$HCO_3^- + H_2O + 2\,e^- \rightarrow HCOO^- + 2\,OH^- \quad (6)$$

To confirm that bicarbonate is reduced, and to also rule out the possibility that the reduction peak is due to the reduction of a copper carbonate layer that has formed in the anodic region of the voltammogram,[22,23] further analysis of the products formed at the reduction peak needs to be done, and this is reported in the next section.

3.3.2 Products formed at the reduction peak

To determine the products formed at the observed reduction peak, measurements with online electrochemical mass spectroscopy (OLEMS) and online HPLC were performed. For both types of experiment, phosphate buffers starting at pH 6.7 and at pH 11.6 were used. In Figures 3.3 and 3.4 the results of

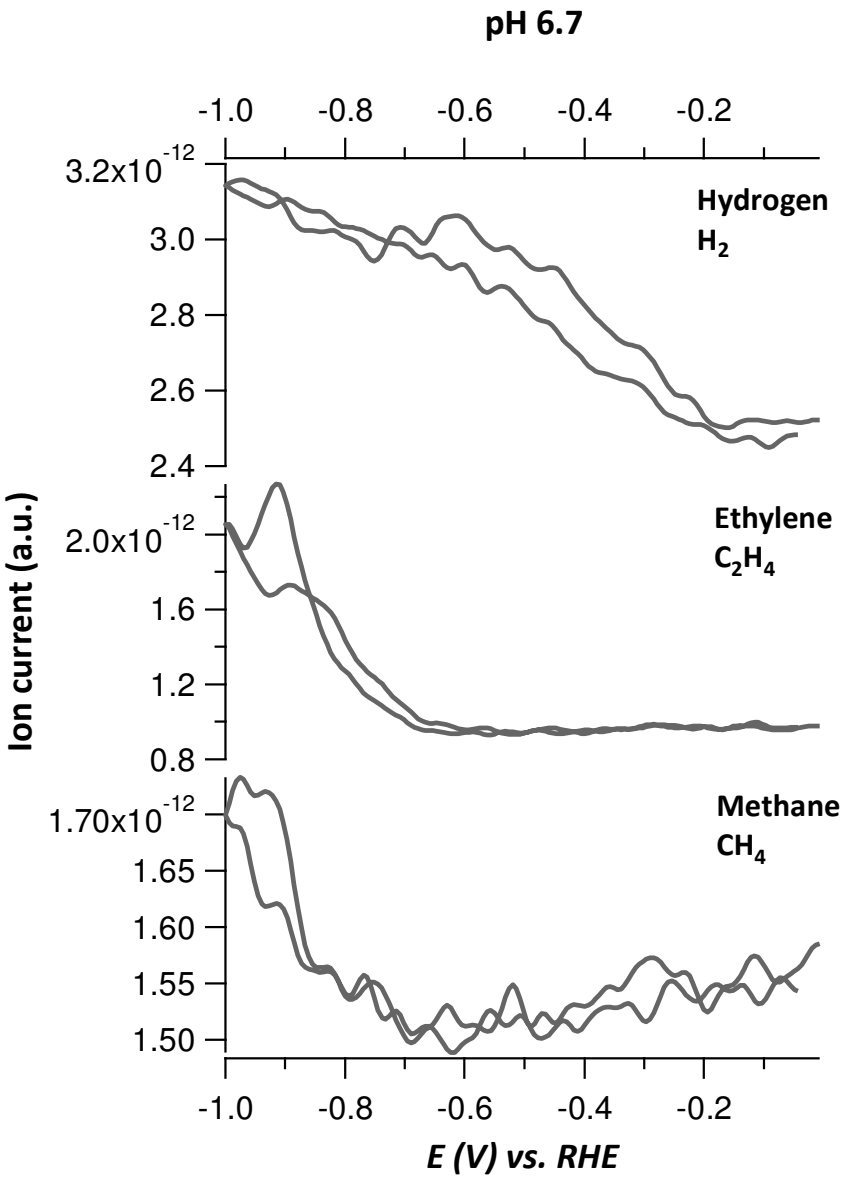

Figure 3.3 Spectra of mass fragments associated with volatile products from CO_2 reduction in a phosphate buffer starting at pH 6.7. Hydrogen production, methane production and ethylene production were measured versus potential by scanning at a scan rate of 1 mV s^{-1} and constant sampling from the surface of the electrode.

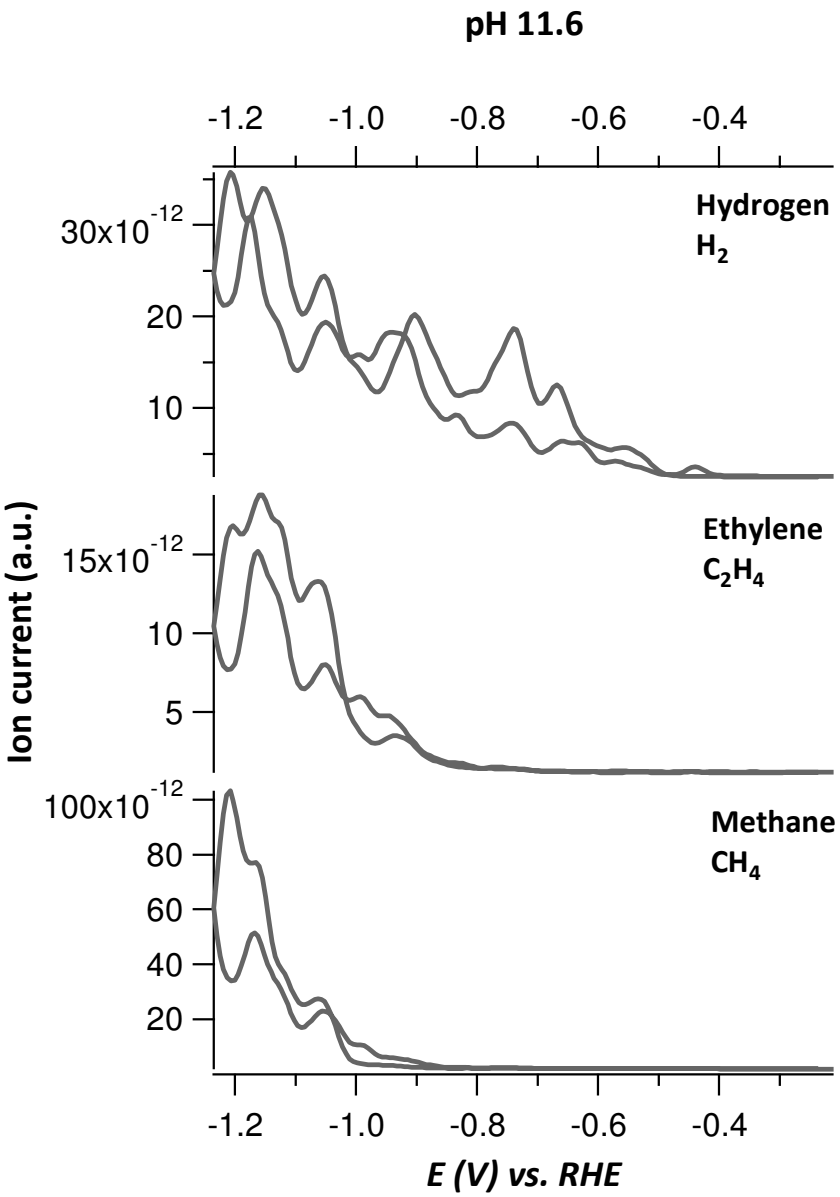

Figure 3.4 Spectra of mass fragments associated with volatile products from CO_2 reduction in a phosphate buffer starting at pH 11.6. Hydrogen production, methane production and ethylene production were measured versus potential by scanning at a scan rate of 1 mV s^{-1} and constant sampling from the surface of the electrode.

the OLEMS measurements are shown. The intensities of the peaks differ due to the position of the OLEMS tip with respect to the electrode, making it difficult to make quantitative conclusions. However, some semi-quantitative differences can be observed from the results in Figures 3.3 and 3.4. Most importantly, the CO_2 reduction from the pH 6.7 phosphate buffer as electrolyte yields no significant amount of methane, while in the electrolyte with a phosphate buffer starting at pH 11.6, methane is the dominant gaseous product with an onset potential of -0.9 V. In both electrolytes ethylene is detected as reduction product, at roughly the same onset potential. Almost no volatile products were detected in the potential range of the low-potential reduction peak (-0.6 V – -0.7 V). However, it should be mentioned that with the OLEMS setup we were unable to measure CO production, since CO_2 fragments into CO in the ion chamber of the mass spectrometer forming CO. Therefore, it is impossible to accurately determine the CO production, though we do assume that CO is formed as an intermediate at the potentials at which methane and ethylene are observed.

Earlier literature reports state that in K_2HPO_4 solutions and relatively concentrated HCO_3^- solutions methane is produced preferentially while in dilute HCO_3^- solutions ethylene is produced preferentially.[14] This is consistent with our

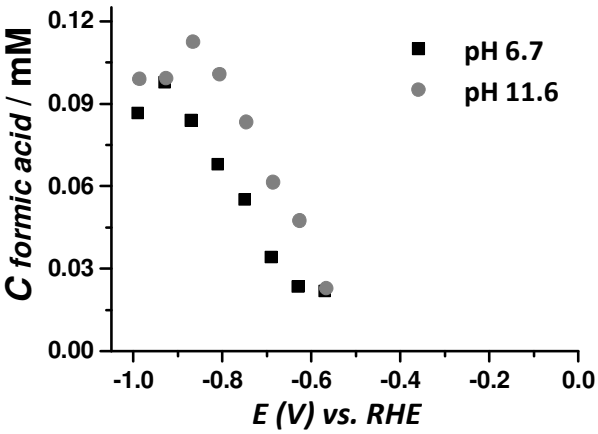

Figure 3.5 Formation of formic acid detected with online HPLC using a phosphate buffer at pH 6.7 (0.1 M KH_2PO_4 + 0.1 M K_2HPO_4) (■) and a phosphate buffer at pH 11.6 (0.1 M K_2HPO_4 + 0.1 M K_3PO_4) (●).

result in terms of the enhanced production of methane in the electrolyte starting at pH 11.6, since this electrolyte contains a relatively high concentration of HCO_3^-.

The results of online HPLC measurements are depicted in Figure 3.5. As can be seen formic acid is detected, but since our eluens used for analysis consisted of a low concentration of sulfuric acid, the actual product formed in the electrochemical cell is not formic acid but formate, which is the preferred form at these pH values. The concentration of detected formate follows the low-potential reduction peak observed in the cyclic voltammetry (Figure 3.1). However, there is not much difference in the onset potential of formate formation between the electrolyte with a phosphate buffer starting at pH 11.6 and a phosphate buffer starting at pH 6.7. The main difference between both buffers is that the production of formate is a little higher in the phosphate buffer starting at pH 11.6. The concentration of formate peaks at a potential at which almost no ethylene or methane is formed. Furthermore, the potential at which formate production peaks agrees well with maximum of the current peak observed in Figure 3.1c. This indicates that the current peak can be ascribed to the selective reduction of CO_2 or bicarbonate to formate and also it indicates that this process could be

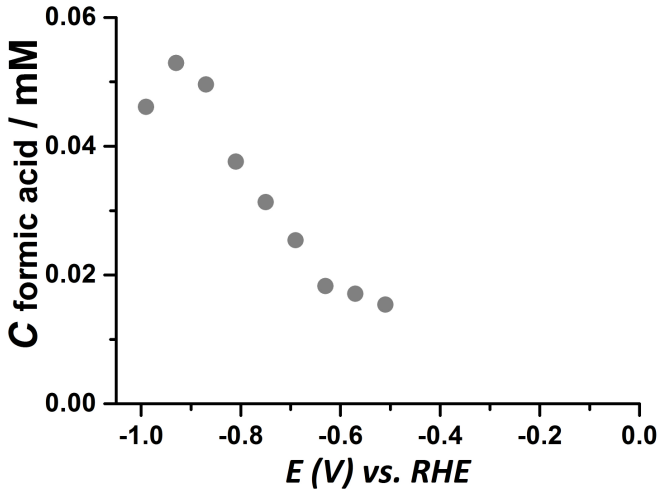

Figure 3.6 Formation of formic acid detected with online HPLC using a 1.0 M $KHCO_3$ electrolyte without purging CO_2.

selective if hydrogen evolution could be suppressed, without formation of CO, which is the precursor for making ethylene and methane.[6,24]

To study if either CO_2 or bicarbonate is the species that is reduced, an online HPLC experiment with a 1.0 M $KHCO_3$ electrolyte without purging CO_2 was performed (Figure 3.6). A cyclic voltammogram of this electrolyte is shown in Figure 3.2. Interestingly, the detection of formic acid, and thus the production of formate, in the electrolyte peaks at approximately the same potential as where the reduction peak in the voltammogram is seen. This experiment implies that bicarbonate and not CO_2 is reduced to formate, similar to what has been suggested for bicarbonate reduction on palladium.[21]

3.3.3. The influence of electrode morphology

Different electrode preparations were tried, to see if they had an influence on the outcome of the reaction. Instead of mechanically polishing the electrode, as was done for the electrodes studied in Figures 3.1-5, the electrode was cleaned with an electropolishing method. The results of cyclic voltammetric measurements with electropolished electrodes were the same as with the mechanically polished electrode.

The electrode was also subjected to a literature procedure described by Chorkendorff et al.[25] to cover the electrode with nanoparticles. As can be seen in Figure 3.7, a significant enhancement of the peak was observed.

Online HPLC measurements indicated that the production of formate increased by a factor of approximately 6. This enhancement can be ascribed to the increased area of the electrode, as it has been reported

that the area increased by a factor of 2-3, estimated from scanning electron microscopy (SEM) images.[25] Rough surfaces, with kinks and steps, can exhibit different selectivities towards products and different efficiencies in CO_2 reduction compared to flat surfaces.[26,27] Since electropolishing generally creates flat

surfaces and a rough surface is created with the procedure used, this may also account for the observed difference in the reduction peak.

To see if the morphology of the flat surfaces, created by electropolishing, and the morphology of the roughened surface, created by the roughening procedure, influences the reduction, and thus the formation of formate, a study using single crystal electrodes was performed. The electrochemical response of the low-index surfaces, Cu(100), Cu(110) and Cu(111), is shown in Figure 3.8a. On the Cu(100) surface the current response is higher than on the Cu(110) and Cu(111) single crystal electrodes, but the formate-related reduction peak is less prominent than on the other two single crystal electrodes. Both observations are explained by a higher activity for the HER at relatively high potentials (> -0.6 V vs. RHE) on the Cu(100) surface as compared to the Cu(110) and Cu(111) surfaces.[28] The surface that exhibits a clear reduction peak is the Cu(110) surface, whereas Cu(100) and Cu(111) exhibit a reduction plateau instead of a reduction peak. This is in accordance with the enhancement of the reduction peak on roughened surfaces, since it is expected that on these surfaces the amount of undercoordinated sites is higher than on the polycrystalline electrodes and

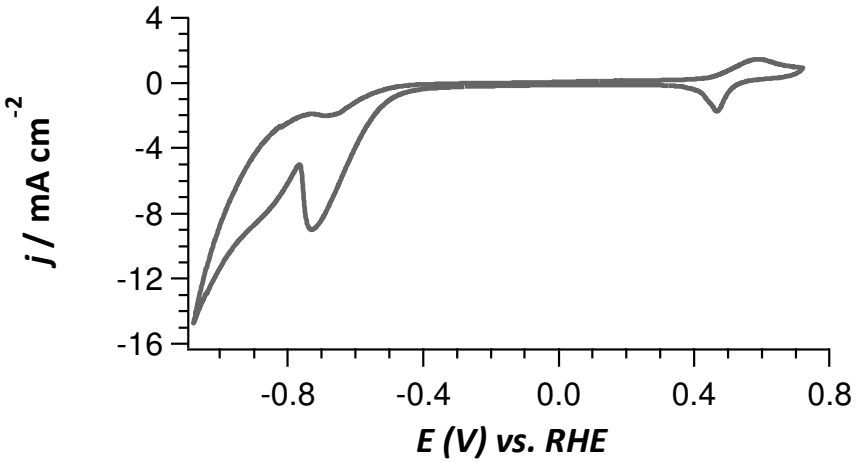

Figure 3.7 Cyclic voltammogram of CO_2 reduction in a phosphate buffer starting at pH 11.6 on a modified Cu electrode at a scan rate of 20 mV s^{-1}.

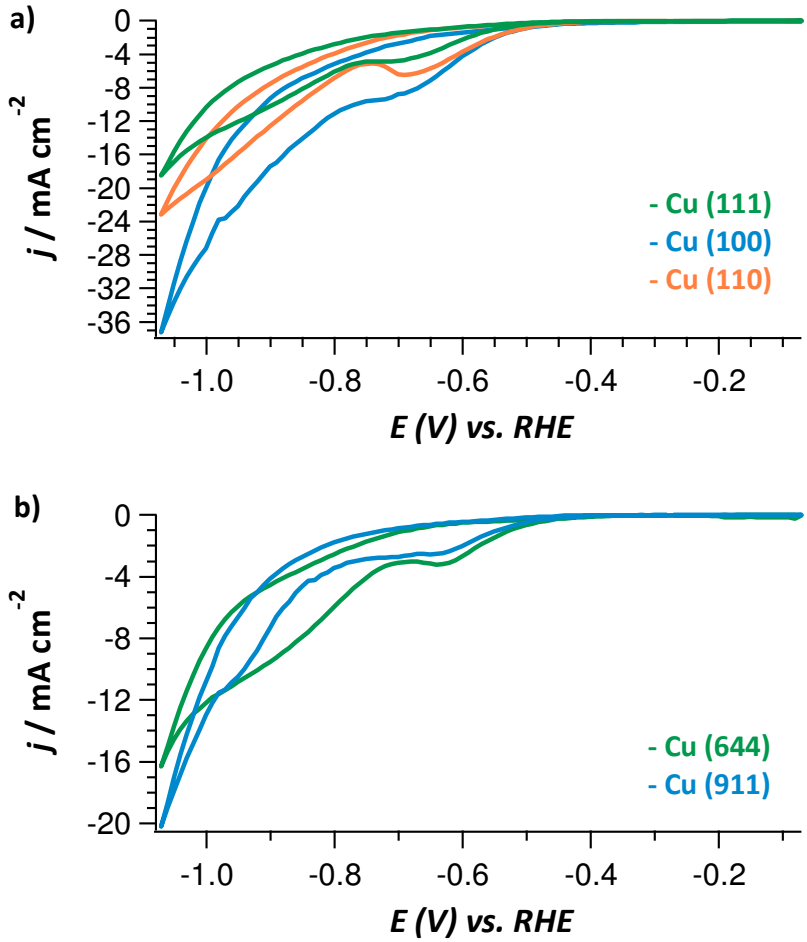

Figure 3.8 Cyclic voltammograms CO_2 reduction in a phosphate buffer starting at pH 11.6 on single crystal electrodes at a scan rate of 20 mV s^{-1}. **a)** Cyclic voltammograms on Cu(111) (green), Cu(100) (blue) and Cu(110) (orange), **b)** Cyclic voltammograms on Cu(644) (green) and Cu(911) (blue).

Cu(110) is the most undercoordinated surface of the three basal surface structures Cu(100), Cu(110) and Cu(111).

To study if steps play a role as undercoordinated sites in the reduction reaction, experiments with stepped surfaces were performed (Figure 3.8b). The Cu(911) [= 4(100) × (111)] surface shows a lower overall activity than the Cu(100) surface. Also it shows an elongated reduction plateau in comparison with Cu(100), however no reduction peak as seen with Cu(110) is observed. For Cu(644) [= 4(111) × (100)] a small reduction peak was observed.

3.3.4 Cation and anion effects on the reduction peak

To investigate the influence of the composition of the electrolyte, different cations and anions were tested in the phosphate buffer system. Different cationic and anionic species have been long known to have an effect on electrochemical processes.[29,30] Earlier studies with different alkaline cations in 0.1 M hydrogen carbonate solutions showed that the current efficiency towards formate increased significantly with Cs^+, while Na^+ and K^+ gave nearly the same current efficiency.[31]

The influence of cations was tested by employing phosphate buffers starting at pH 11.6 with different cations. The resulting voltammetry is shown in Figure 3.9. Unfortunately, Li^+ could not be included since Li_2HPO_4 / Li_3PO_4 is not soluble in water. Figure 3.10 shows that the Na^+ containing buffer shows similar behavior as the K^+ containing buffer. Cs^+ and Rb^+ buffers, however, behave somewhat differently. Both buffers show a reduction peak, but the peak current for Rb^+ is lower than for the other alkali cations.

Cation effects are often explained in the light of the extent of hydration of the cationic species. This extent of hydration determines if the cation is adsorbed at the electrode or not.[31,32] Small cations, such as Li^+ and Na^+ are strongly hydrated and will not adsorb, while larger cations like K^+, Rb^+ and Cs^+ will preferentially adsorb. This will thus influence the selectivity of the systems in CO_2 reduction. However, such an effect is not clearly visible from Figure 3.9, although

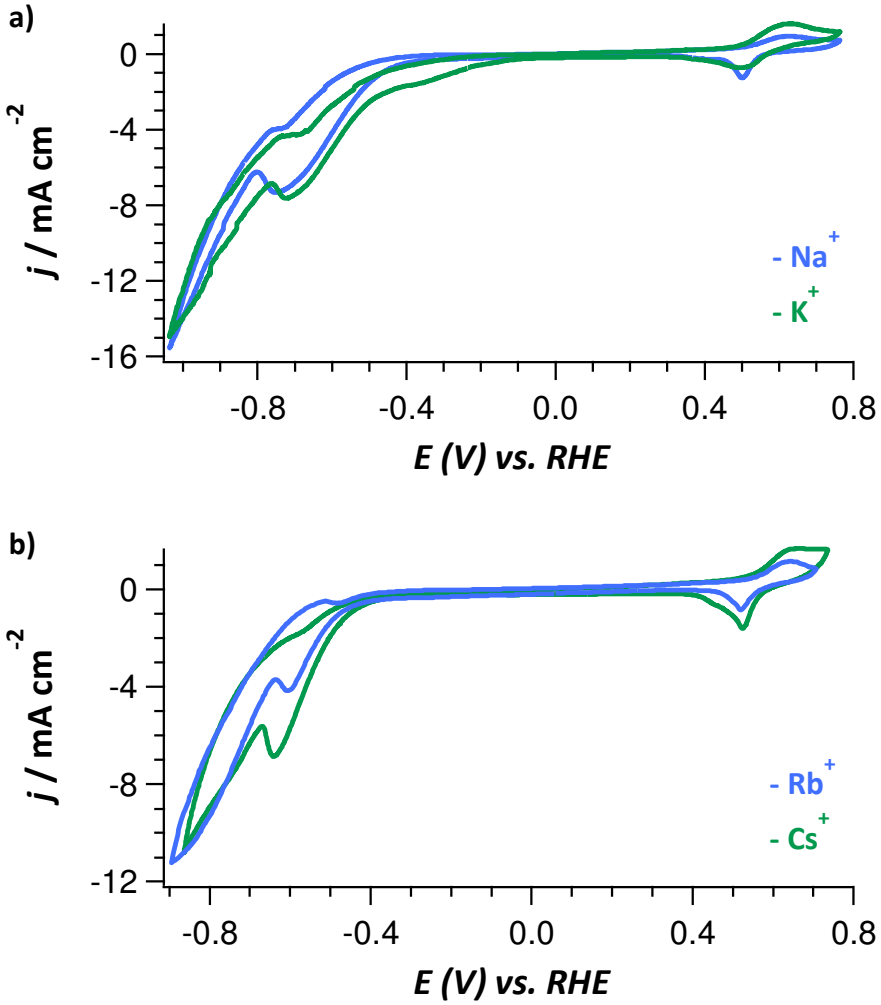

Figure 3.9 a) Cyclic voltammograms of CO_2 reduction in 0.1 M Na_2HPO_4 / 0.1 M Na_3PO_4 (blue) and 0.1 M K_2HPO_4 / 0.1 M K_3PO_4 (green) at a scan rate of 20 mV s^{-1}; **b)** Cyclic voltammograms of CO_2 reduction in 0.1 M Rb_2HPO_4 / 0.1 M Rb_3PO_4 (blue) and 0.1 M Cs_2HPO_4 / 0.1 M Cs_3PO_4 (green) at a scan rate of 20 mV s^{-1}.

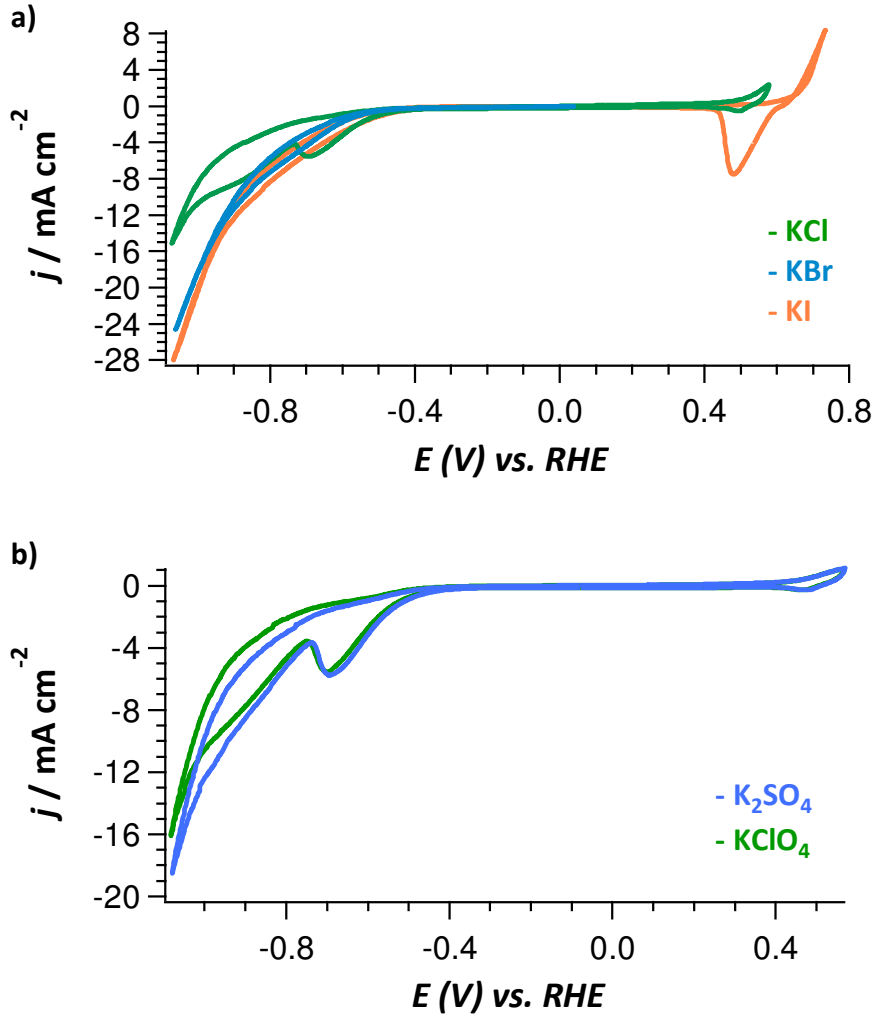

Figure 3.10 a) Cyclic voltammograms of CO_2 reduction in 0.1 M K_2HPO_4 / 0.1 M K_3PO_4 with 0.1 M KI (orange), KBr (blue) and KCl (green) at a scan rate of 20 mV s^{-1}; **b)** Cyclic voltammograms of CO_2 reduction in 0.1 M K_2HPO_4 / 0.1 M K_3PO_4 with 0.1 M $KClO_4$ (green) and KSO_4 (blue) at a scan rate of 20 mV s^{-1}.

Rb^+ seems to be somewhat different compared to the other alkali metal buffers. For the reduction of HCO_3^- on Pd it is reported that the use of Cs^+ enhances the faradaic efficiency significantly,[21] but this is not observed in this reduction reaction on Cu.

The influence of anions was studied with 0.1 M KCl, KBr, KI and 0.1 M $KClO_4$ and K_2SO_4 in a phosphate buffer at pH 11.6 (0.1 M K_2HPO_4 + 0.1 M K_3PO_4). The results are depicted in Figure 3.10. A clear trend in the series with potassium halide salts can be observed. While the addition of KCl to the electrolyte does not affect the appearance of the reduction peak, addition of KBr and KI to the electrolyte does. In both cases the reduction peak is not seen anymore. The reduction currents with KBr and KI in the electrolyte are also higher than seen in electrolytes with less strongly adsorbing anions, especially for potentials lower than -0.6 V, suggesting that the presence of strongly adsorbing anions promotes the activity for hydrogen evolution. The results of the reduction reaction with 0.1 M $KClO_4$ and KSO_4 added to the electrolyte show very similar behaviour (Figure 3.10b): both anions show the reduction peak with a similar intensity as seen before.

We conclude that there is a strong effect of the anion species in the electrolyte on the overall reaction. Anions that are known to be strongly adsorbed on electrode surfaces, such bromide and iodide, appear to block the reduction reaction and thus formate production, and they specifically favor hydrogen evolution. Surprisingly, this effect is very significant at these rather negative potentials, and at this moment it would be difficult to say whether the effect is directly attributable to specific anion adsorption.

3.4 Conclusions

The electrochemical reduction of CO_2 on a copper electrode in alkaline phosphate buffers was investigated. Our specific attention was focused on a reduction peak at relatively low potential (-0.6 – -0.7 V vs. RHE, at the foot of the overall reduction wave) that was previously ascribed to the formation of a CO ad-layer on the electrode. Our online HPLC measurements show that this peak is not due to the formation of a CO ad-layer but rather due to the selective direct reduction of

bicarbonate to formate. Online mass spectrometry experiments show that volatile products such methane and ethylene, which require CO as an intermediate, are formed at more negative potentials. Furthermore, we have shown that the reduction of HCO_3^- on a copper electrode can be influenced by anionic and cationic species present in the electrolyte, and the reduction can be boosted by roughening the surface of the electrode. Since no other products were detected, this process could be made selective as long as the HER is sufficiently suppressed. Reduction of 'stored CO_2', i.e. HCO_3^- in this case, could thus also be a step towards renewable energy since formic acid is a potential feedstock for fuel cells.

References

(1) Gattrell M.; Gupta N.; Co A. *Energy. Convers. Manage*. **2007**, *48*, 1255-1265.

(2) Whipple D.T.K.; Kenis P.J.A. *J. Phys. Chem. Lett*. **2010**, *1*, 3451-3458.

(3) Hori Y.; Kikuchi K.; Suzuki S. *Chem. Lett.* **1985**, *11*, 1695-1698.

(4) Scibioh M.A.V.; Viswanathan B. *Proc. Indian Natn. Sci. Acad. A* **2004**, *70*, 1-56.

(5) Gattrell M.; Gupta N.; Co A. *J. Electroanal. Chem*. **2006**, *594*, 1-19.

(6) Y. Hori in *Modern Aspects of Electrochemistry*, Vol. 42 (Eds: C.G. Vayenas, R.E. White, M.E. Gamboa-Aldeco), Springer, New York, 2008, pp. 89-189.

(7) Spinner N.S.; Vega J.A.; Mustain W.E. *Catal. Sci. Technol.* **2012**, *2*, 19-28.

(8) Schouten K.J.P.; Qin Z.; Pérez Gallent E.; Koper M.T.M. *J. Am. Chem. Soc.* **2012**, *134*, 9864-9867.

(9) Hori Y.; Takahashi R.; Yoshinami Y.; Murata A. *J. Phys. Chem. B* **1997**, *101*, 7075-7081.

(10) Jović V.D.; Jović B.M. *J. Electroanal. Chem.* **2003**, *541*, 13-21.

(11) Wonders A.H.; Housmans T.H.M.; Rosca V.; Koper M.T.M. *J. Appl. Electrochem.* **2006**, *36*, 1215-1221.

(12) Kwon Y.; Koper M.T.M. *Anal. Chem.* **2010**, *82*, 5420-5424.

(13) Hori Y.; Murata A.; Takahashi R.; Suzuki S. *J. Chem. Soc., Chem. Commun.* **1988**, *1*, 17-19.

(14) Hori Y.; Murata A.; Takahashi R. *J. Chem. Soc., Faraday Trans.* **1989**, *1*, 2309-2326.

(15) De Jesus-Cardona H.D.M.; Del Moral C.; Cabrera C.R. *J. Electroanal. Chem.* **2001**, *513*, 45-51.

(16) Christophe J.; Doneux Th.; Buess-Herman C. *Electrocatal.* **2012**, *3*, 139-146.

(17) Spichiger-Ulmann M.; Augustynsky J. *J. Chem. Soc., Faraday Trans.* **1985**, *181*, 713-716.

(18) Podlovchenko B.I.; Kolyadko E.A.; Lu S. *J. Electroanal. Chem.* **1994**, *373*, 185-187.

(19) Teeter T.E.; Van Rysselberghe P. *J. Chem. Phys.* **1954**, *22*, 759-760.

(20) Hori Y.; Suzuki Sh. *J. Electrochem. Soc.* **1983**, *130*, 2387-2390.

(21) Spichiger-Ulmann M.; Augustynski J. *Helv. Chim. Acta* **1986**, *69*, 632-634.

(22) Perez Sanchez M.; Souto R.M.; Barrera M.; Gonzalez S.; Salvarezza R.C.; Arvia A.J. *Electrochim. Acta* **1993**, *38*, 703-715.

(23) Smith B.D.; Irish D.E. *J. Electrochem. Soc.* **1997**, *144*, 4288-4296.

(24) Schouten K.J.P., Kwon Y., van der Ham C.J.M., Qin Z., Koper M.T.M. *Chem. Sci.* **2011**, *2*, 1902-1909.

(25) Tang W.; Peterson A.A.; Varela A.S.; Jovanov Z.P.; Bech L.; Durand W.J.; Dahl S.; Norskov J.K.; Chorkendorff I. *Phys. Chem. Chem. Phys.* **2012**, 14:76-81

(26) Hori Y.; Takahashi I.; Koga O.; Hoshi N. *J. Mol. Catal. A: Chem*. **2003**, *199*, 39-47.

(27) Takahashi I.; Koga O.; Hoshi N.; Hori Y. *J. Electroanal. Chem.* **2002**, *533*, 135-143.
(28) Brisard G.; Bertrand N.; Ross P.B.; Marković N.M. *J. Electroanal. Chem*. **2000**, *480*, 219-224.
(29) Delahay P.; Mattax C. *J. Am. Chem. Soc.* **1954**, *76*, 5314-5318.
(30) Frumkin A.N. *Trans. Faraday Soc.* **1959**, *55*, 156-167.
(31) Murata A.; Hori Y. *Bull. Chem. Soc. Jpn.* **1991**, *64*, 123-127.
(32) Kaneco S.; Katsumata H.; Suzuki T.; Ohta K. *Electrochim. Acta* **2006**, *51*, 3316-3321.